
The Eurasia Proceedings of Science, Technology, Engineering & Mathematics (EPSTEM)

Volume 1, Pages 41-51

ICONTES2017: International Conference on Technology, Engineering and Science

ANALYSIS OF THE TEMPERATURE EFFECT ON THE PLASTIC STRAIN OF POLYMERS DURING HIGH PRESSURE TORSION (HPT) PROCESS

Ahmed Draï

Department of Mechanical engineering Mustapha Stambouli University of Mascara

Benaoumeur Aour

Laboratory of Applied Biomechanics And Biomaterials (LABAB), National Polytechnic School of Oran

Abstract: The high pressure torsion (HPT) is an efficient process to obtain enhanced microstructures via super-plastic deformation. In view of its optimization, it is of prime importance to assess the relationships between processing conditions and material flow. More precisely, detailed knowledge of the plastic strain distribution in the deformed material in relation to HPT processing variables is very useful. In this context, the present work is focused primarily to highlight the effect of the temperature on the plastic strain distribution into the processed polymers by HPT. The effect of the sample thickness is also studied. To this end, the material parameters of an elasto-viscoplastic phenomenological model were derived from compressive tests at different temperatures and strain rates on a typical thermoplastic polymer (high density polyethylene (HDPE)). The distribution of the equivalent plastic strain and the loading conditions were analysed. Recommendations on process conditions were proclaimed at the end of this work.

Keywords: HPT, HDPE, finite element, plastic strain, temperature.

| Nomenclature | |
|---------------------|---|
| b | Hardening parameter |
| \mathbf{C} | Fourth-order isotropic elastic modulus tensor |
| c_{ij} | A tensor dependent on the location of the field point x_f |
| \mathbf{d} | Strain rate tensor |
| d | Distance along sample thickness from the bottom |
| \mathbf{d}^e | Elastic part of strain rate tensor |
| \mathbf{d}^{vp} | Viscoplastic part of strain rate tensor |
| E | Young's modulus |
| h | Hardening parameter |
| k | Initial yield stress in Chaboche model |
| K, n | Viscosity parameters |
| \mathbf{W} | Spin tensor |
| δ_{ij} | Kronecker-delta symbol |
| $\{\varepsilon\}$ | Strain vector |
| ε_0 | Initial yield strain |
| ε^p | Equivalent plastic strain |
| $\dot{\varepsilon}$ | Strain rate |
| λ, μ | Lame's constants |

Introduction

Severe Plastic Deformation (SPD) has attracted a great deal of work over the past two decades because of the materials' enhanced properties. Different techniques of SPD have been used to alter the microstructure by inducing large plastic strain into the materials. Among them, we can cite, Equal Channel Angular Pressing/Extrusion (ECAP/ECAE) [11], High Pressure Torsion (HPT) [14], Accumulative Roll Bonding (ARB) [10], Cyclic Extrusion Compression (CEC) [9], Repetitive Corrugation and Straightening (RCS) [6], etc. Based on the extensive research conducted to date, applications of SPD techniques are now starting to emerge for use in manufacturing industries and several commercial products such as sputtering targets, fasteners and dental implants, are already available.

The most popular SPD processes are equal channel angular pressing (ECAP) and high pressure torsion (HPT). The ECAP process involves simple shear deformation that is achieved by pressing the sample through a die containing two channels of equal cross-section that meet at a predetermined angle. Deformation occurs in the immediate vicinity of the plane lying at the intersection of two channels [12], whereas, the high pressure torsion (HPT) refers to processing that evolved from Bridgman's anvils involves a combination of high pressure with torsional straining (Fig. 1). Today this technique is appreciated by many researchers as the one that allows the most efficient nanostructure materials.

An important issue for many SPD processing schemes, including HPT, is the non-uniformity of plastic deformation. For instance, during HPT straining, the shear strain at the rotation axis should be zero, increasing linearly in the radial direction if the geometry of the sample does not change. This means that the material near the rotation axis of the sample should stay undeformed. This is not supported by numerous micro-structural observations and micro hardness measurements showing a reasonably uniform distribution of micro-hardness, provided the compressive pressure and the torsion angle of the anvil are sufficiently large [8].

The finite element method (FEM) has been widely used for various analyzing forming processes [7], [1], [3], [5]. The method provides detailed information concerning the distribution of strains, strain rates, stresses and material flow, as well as the necessary external loads. The purpose of this work is to determine the optimal processing conditions in the case of polymeric material subjected to large strain due to HPT process. The effect of the sample thickness and the temperature on the plastic deformation behavior were studied in detail. Concluding remarks have been proclaimed at the end of this work.

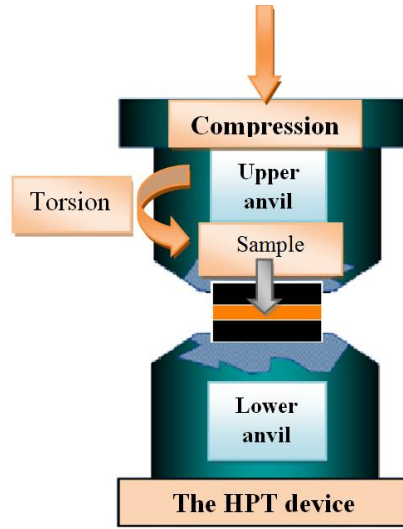


Figure 1. Principle of high pressure torsion process (HPT)

Constitutive Model

The large plastic deformation of the polymer under study (HDPE) is characterized by a strain rate dependent yield followed by a strain hardening. Various constitutive laws, basing on micromechanical or phenomenological considerations [4], [13], were developed to describe the specific behavior of polymers. In this paper, a phenomenological constitutive model was used to describe the behavior of the studied material [2]. It is based on the additive decomposition of the strain rate tensor \mathbf{d} into an elastic part \mathbf{d}^e and a viscoplastic part \mathbf{d}^{vp} as:

$$\mathbf{d} = \mathbf{d}^e + \mathbf{d}^{vp} \quad (1)$$

The elastic strain rate tensor \mathbf{d}^e is given by :

$$\mathbf{d}^e = \mathbf{C}^{-1} \tilde{\boldsymbol{\sigma}} \quad (2)$$

$$\tilde{\boldsymbol{\sigma}} = \dot{\boldsymbol{\sigma}} - \mathbf{W}\boldsymbol{\sigma} + \boldsymbol{\sigma}\mathbf{W} \quad (3)$$

where $\tilde{\boldsymbol{\sigma}}$ is the Jaumann derivative of the Cauchy stress tensor $\boldsymbol{\sigma}$ based upon the spin tensor \mathbf{W} and \mathbf{C} is the fourth-order isotropic elastic modulus tensor:

$$C_{ijkl} = \frac{E}{2(1+\nu)} \left[(\delta_{ik}\delta_{jl} + \delta_{il}\delta_{jk}) + \frac{2\nu}{1-2\nu} \delta_{ij}\delta_{kl} \right] \quad (4)$$

where E , ν and δ are respectively Young's modulus, Poisson's ratio and Kronecker-delta symbol.

The viscoplastic strain rate tensor \mathbf{d}^{vp} can be expressed by the following relationships:

$$\mathbf{d}^{vp} = \frac{3}{2} \left\langle \frac{\sigma_e - R}{K} \right\rangle^n \frac{\boldsymbol{\sigma}'}{\sigma_e} \quad (5)$$

$$\boldsymbol{\sigma}' = \boldsymbol{\sigma} - \text{tr}(\boldsymbol{\sigma})/3 \mathbf{I} \quad (6)$$

$$\sigma_e = \sqrt{3/2 \boldsymbol{\sigma}' \boldsymbol{\sigma}'} \quad (7)$$

where K and n are the viscosity parameters, $\boldsymbol{\sigma}'$ is the deviatoric stress tensor, σ_e is the equivalent stress, and R is the isotropic hardening defined by a simple phenomenological evolution law as follows:

$$R = h \left(1 + \frac{\varepsilon^p}{\varepsilon_0} \right)^m \quad (8)$$

$$\varepsilon^p = \int_0^t \dot{\varepsilon}^p d\tau = \int_0^t \sqrt{2/3 \mathbf{d}^{vp} \mathbf{d}^{vp}} d\tau \quad (9)$$

with ε^p is the equivalent viscoplastic strain, ε_0 is the initial yield strain, m and h are the hardening parameters.

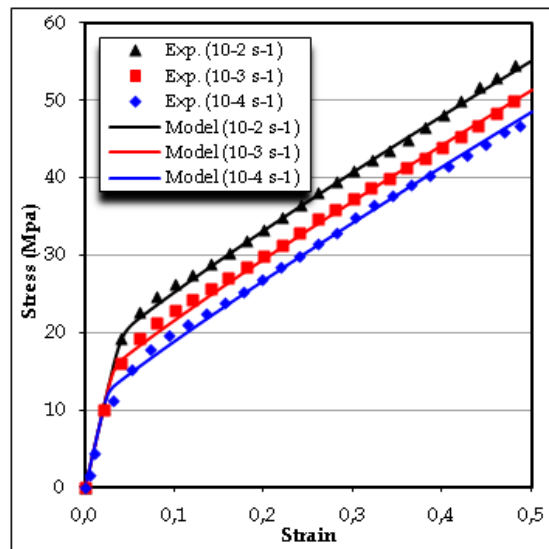
Fitting Experimental Data

In order to simulate the elasto-viscoplastic behavior of HDPE during HPT process, a series of compressive tests at different temperatures ($T=25, 40, 60$ and 80°C) and strain rates ($10^{-2}, 10^{-3}$ and 10^{-4} s^{-1}) were carried out to determine the parameters of the constitutive model presented in the previous section. Indeed, in addition to the Young's modulus and Poisson's ratio, the constitutive equations contain four parameters to be determined: K , n , m and h . The experimental tests have been performed on an electromechanical Instron testing machine using cylindrical samples of 10mm (diameter) \times 10mm (length). During the tests, the values of displacement, loads and time were recorded by the computer using Bluehill software. It is worth noting that Young's modulus E was obtained at low stresses and strains and Poisson's ratio ν was fixed to 0.38 according to the data sheet of the material. The parameters K, n, m and h were determined using a least squares regression fitting and their values are presented in table 1.

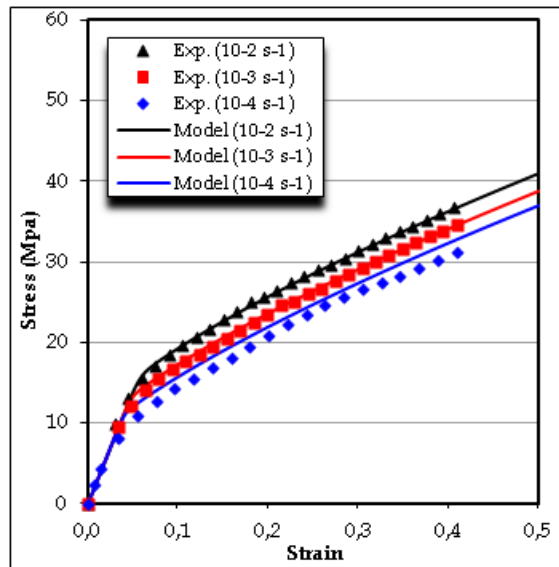
Table 1. The material parameters for HDPE at different temperatures

| T (°C) | E (Mpa) | K (Mpa) | n (-) | h (Mpa) | m (-) |
|-----------|------------|------------|----------|------------|----------|
| 25 | 500 | 31.2 | 7.8 | 3.15 | 0.88 |
| 40 | 280 | 20 | 8.3 | 5 | 0.7 |
| 60 | 150 | 10.7 | 10.2 | 5.5 | 0.65 |
| 80 | 130 | 5.7 | 11.17 | 6 | 0.45 |

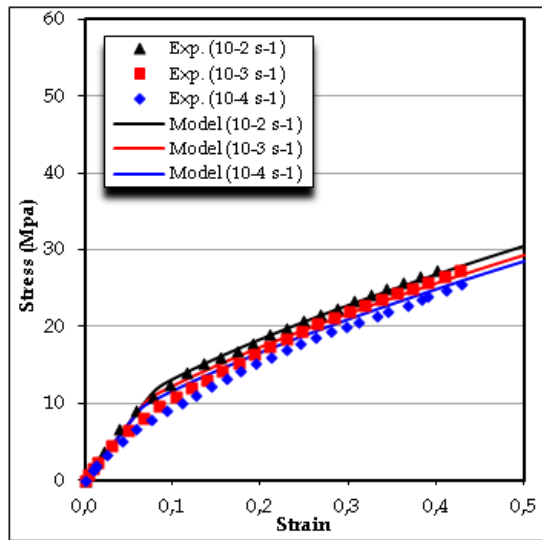
Figure 2 gives the comparison between the experimental data (in circle marker) and the elasto-viscoplastic constitutive model (in solid line) for HDPE at 25°C (Fig. 2a), 40°C (Fig. 2b), 60°C (Fig. 2c) and 80°C (Fig. 2d). It is also noteworthy that, since the model does not include the viscosity effect, an average value of E was adopted for each temperature in the numerical computations.



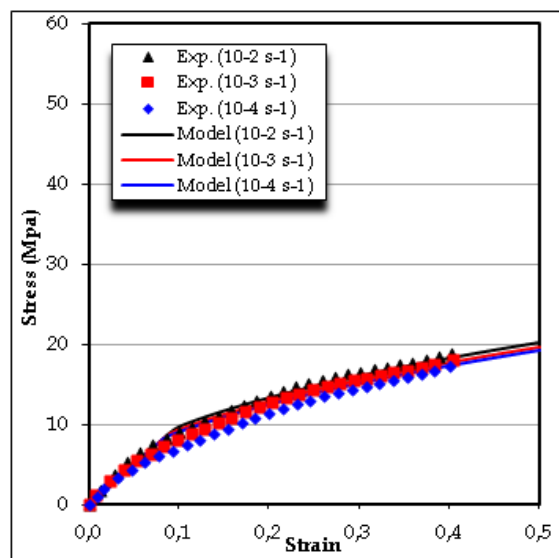
(a)



(b)



(c)



(d)

Figure 2. Stress-strain curves of HDPE for various temperatures: (a) room temperature (25 °C), (b) 40 °C, (c) 60 °C, (d) 80 °C.

Finite Element Analysis of HPT Process

The simulations were performed using the finite element software MSC.Marc. The initial dimensions of the HDPE sample are 10 mm (diameter) \times 10 mm (height) (Fig. 3). The upper and lower anvils were considered as rigid bodies in the modeling. In the first step, an imposed vertical displacement was assigned to the upper anvil in the compressive direction and was maintained during the second step of the torsion.

Meshes Sensitivity

Theoretically, for reasons of symmetry in the loading and geometry of the sample, only a quarter instead of the full sample (Fig.3) can be modeled. This enables us to save enormously the computing time. But, from a practical point of view, before simulating HPT process, it is useful to confirm whether the use of a sample quarter does not affect considerably the reliability of the results. To this end, a comparison between the results obtained using both geometries with different meshes has been presented. The samples were meshed using eight-node isoparametric hexahedral elements and the same process conditions were used for the six meshes.

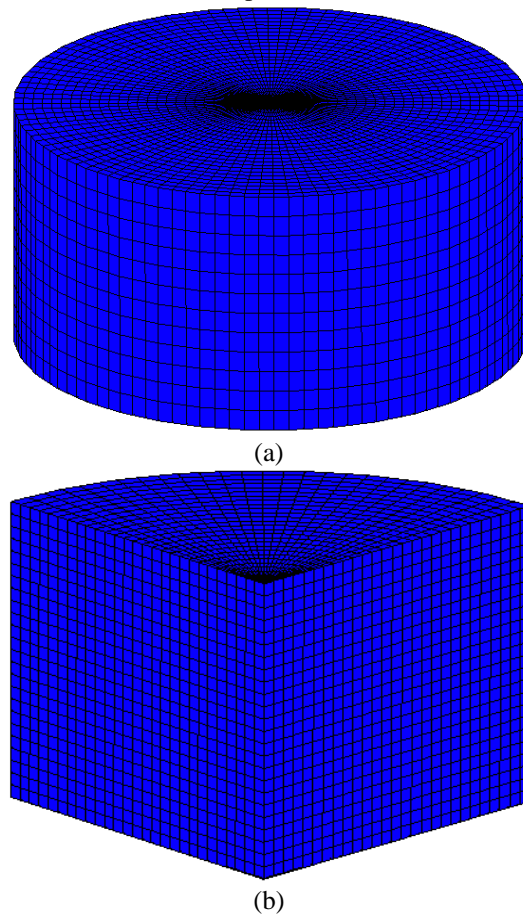


Figure 3. Finite element discretization of: (a) a complete disc, and (b) a quarter of the disc.

Figure 4 illustrates a comparison of the equivalent plastic strain distribution along the radial distance for the six meshes at the end of HPT process with an imposed compressive displacement of 1 mm and a torsion angle of 60°. It can be seen that there is a good agreement between the results obtained by the both geometries when the same size of the element is used for a quarter of the disc and a full disc. However, a slight difference has been highlighted when the radial distance r is between 8 and 10mm. The CPU time for a quarter of the disc (QD) and the full disc (FD) is illustrated in figure 5. It can be seen that the CPU time increases significantly with the increase of the number of elements. Indeed, the CPU time for the fine mesh is about six times of that of the coarse mesh in the case of QD and 12 times in the case of FD. Therefore, in order to obtain a best compromise between precision and computation time, in what follows, we use a quarter of the disc with a fine mesh. This allows us to improve the exactitude without a significant increase of the CPU time.

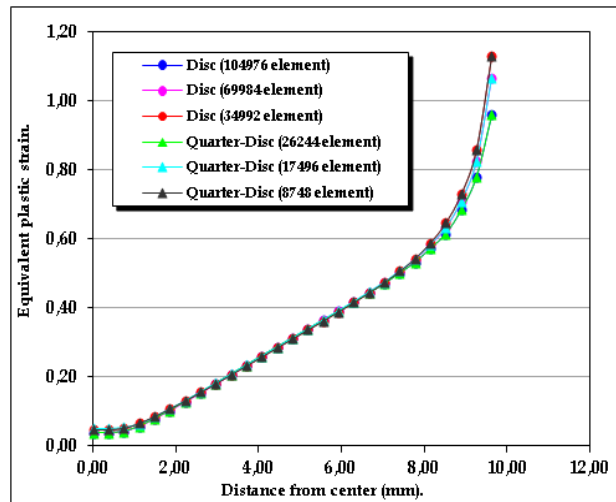


Figure 4. Comparison of the equivalent plastic strain distribution along the radial distance for the six meshes at the end of HPT process.

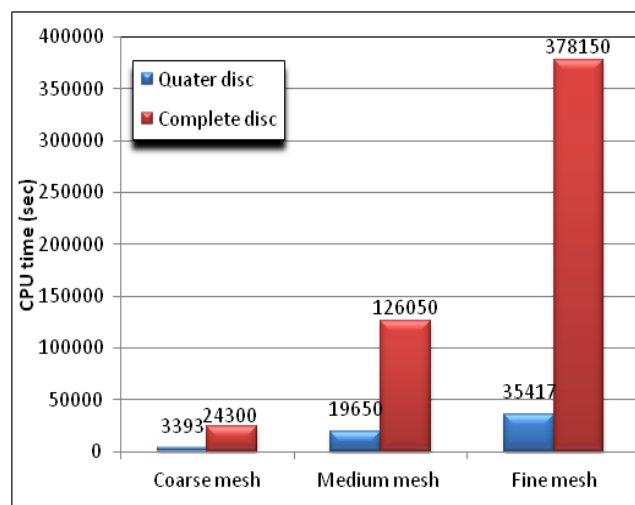


Figure. 5 Comparison of the CPU time for different meshes at the end of HPT process.

Effect of the Sample Thickness

The evolution of the equivalent plastic strain distribution along the radial distance of the HDPE sample is shown in Fig. 6 for three different thicknesses $t = 5, 7$ and 10 mm. A vertical displacement of 1mm with a linear speed of 0.2mm/s and a torsion angle of 30° with an angular velocity of 0.0523 rad/s) have been employed. It can be seen, that the equivalent plastic strain decreases with the increase of the sample thickness.

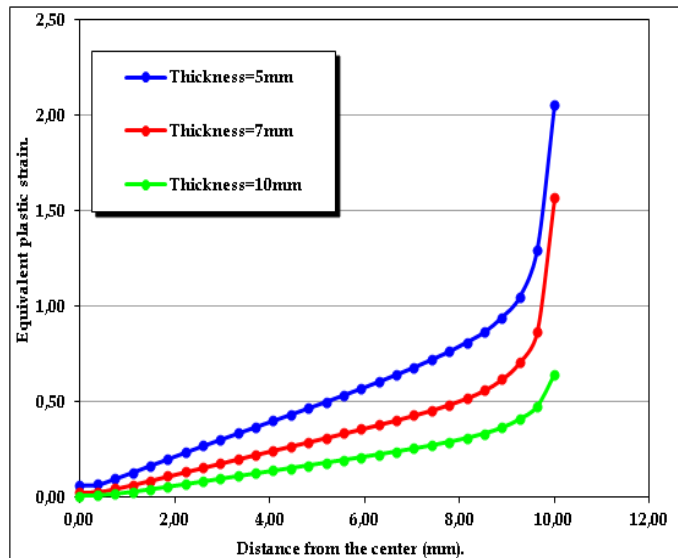


Figure 6. Effect of the sample thickness on the evolution of the equivalent plastic strain

Figure 7 shows the plastic strain distribution for two different thicknesses of 5 and 10 mm. In order to compare the levels of plastic deformation, the first one ($t=5\text{mm}$) is deformed by a torsion angle of 30° and the second one ($t=10\text{mm}$) is deformed using different torsion angles ($\theta=30, 60, 90$ and 120°). It can be observed that to obtain the same level of plastic strain, the sample with a thickness of 10mm must be deformed by a torsion angle equal to three times of that with a thickness of 5mm. This can be clearly shown by plotting the contour plots of the equivalent plastic strain distributions for each thickness as shown in Fig. 8.

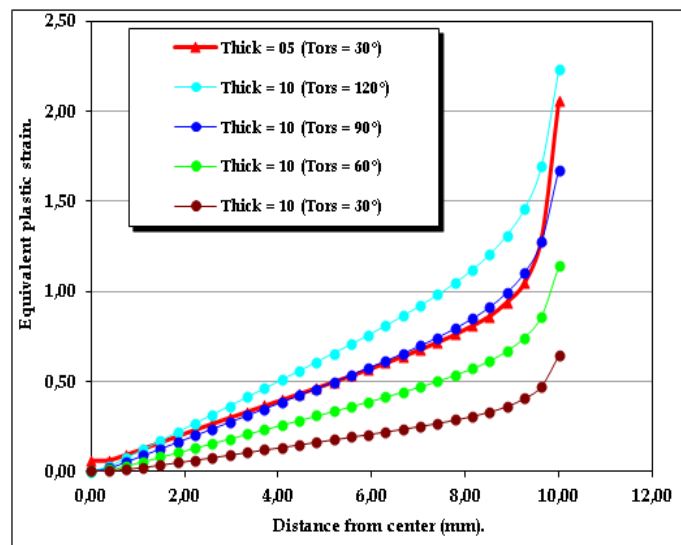
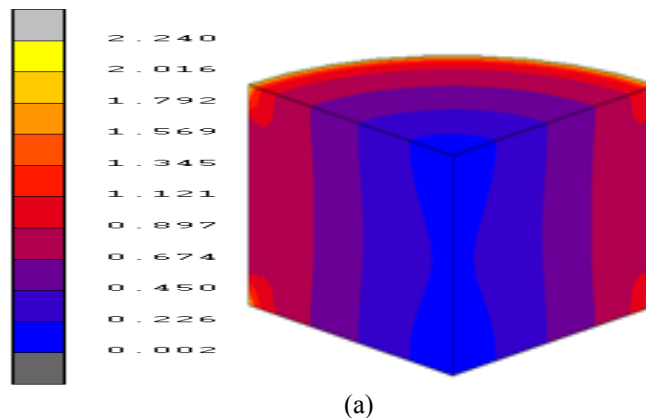
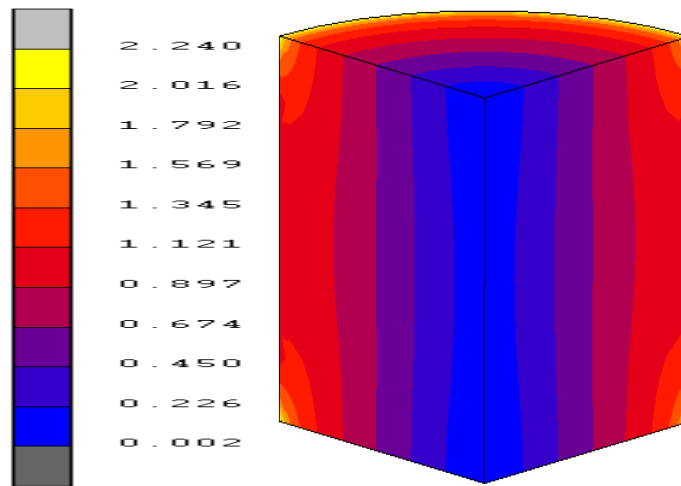


Figure 7. Evolution of the equivalent plastic strain in the case of a thickness of 5mm with a torsion angle of 30° and a thickness of 10mm with different torsion angles.





(b)

Figure 8. Equivalent plastic strain contours in the case of (a) a sample with a thickness of 5 mm deformed by a torsion angle of 30° and (b) a sample with a thickness of 10 mm deformed by a torsion angle of 90°.

Temperature Effect

In order, to study the dependence of the polymer behaviour during HPT process in terms of the temperature, a series of numerical computations under isothermal conditions was carried out for four different temperatures $T = \{25, 40, 60 \text{ and } 80 \text{ }^\circ\text{C}\}$. Noting that the same constitutive model has been identified at different temperatures under isothermal conditions and the obtained material parameters are presented in Table 1. An imposed compressive displacement of 2.5 mm with a speed of 0.5 mm/s followed by a torsion angle of 30° with an angular velocity of 0.26 rad/s were applied on the sample by the upper anvil.

Distribution of the Equivalent Plastic Strain

Figure 9 shows the contour plots of the equivalent plastic strain distribution into the HDPE samples at $T = 25^\circ\text{C}$ (Fig. 9a), 40°C (Fig. 9b), 60°C (Fig. 9c) and 80°C (Fig. 9d). According to these plots, it appears that the equivalent plastic strain is higher at the outer region and lower at the central region since the material at the outer region flows faster than that of the central zone. This aspect can be clearly seen by representing the evolution of the total equivalent plastic strain along the radial distance for different temperatures (Fig. 10).

Furthermore, it can be observed that the temperature strongly influences the magnitude of the equivalent plastic strain. Indeed, the higher is the temperature; the lower is the plastic strain. In addition, one can notice that the distribution of the plastic strain is highly temperature sensitive at low temperatures, whereas this effect becomes insignificant beyond a certain temperature as illustrated in Fig. 10, since the results at 60°C and 80°C are almost identical.

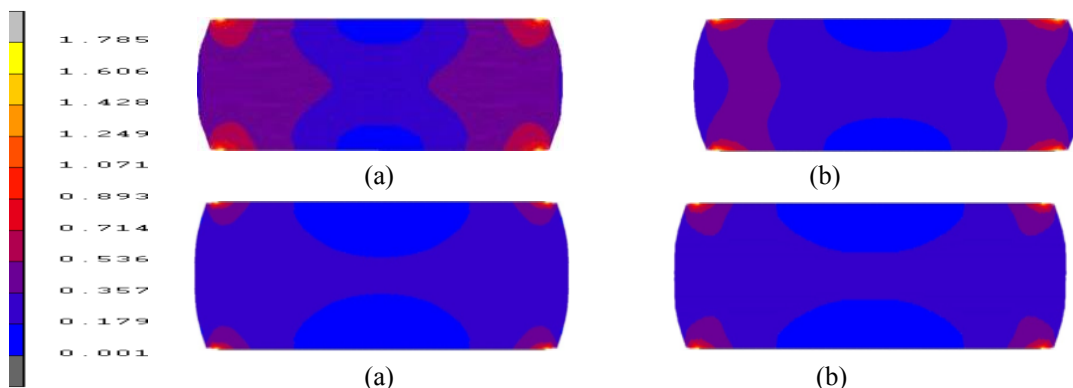


Figure 9. Equivalent plastic strain contours in the case of (a) a sample with a thickness of 5 mm deformed by a torsion angle of 30° and (b) a sample with a thickness of 10 mm deformed by a torsion angle of 90°.

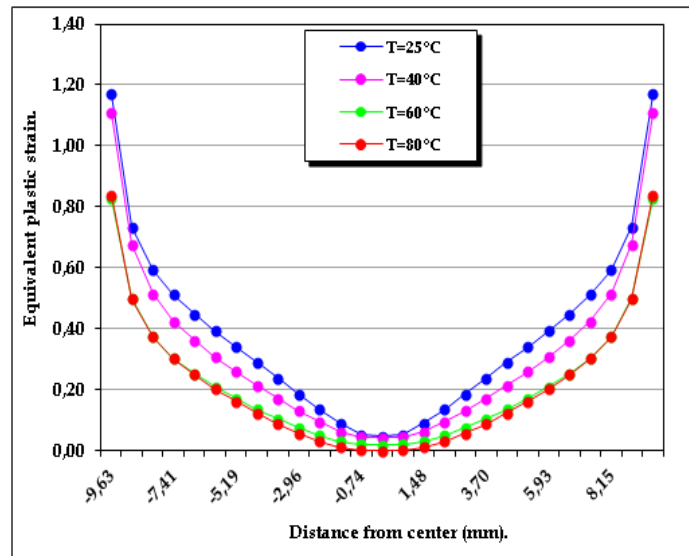


Figure 10. Evolution of the equivalent plastic strain along the radial distance of the disc for different temperatures

Distribution of the Pressing Force

Figure 11 shows the actual values of the pressing force applied by the upper anvil during HPT process of HDPE samples at various temperatures. The pressing force required for each temperature in the ascending order (25, 40, 60 and 80°C) is respectively 21.7, 16.8, 11.5, and 8.25kN. One can see that the higher is the temperature; the lower is the required pressing force. Another interesting point is the evolution of the force versus time during the process, which can be subdivided into two main stages. The first stage starts from the origin up to the maximum. This stage corresponds to the compressive phase. The second stage corresponds to the decrease of the load from the peak to the minimum. This stage corresponds to the torsion phase which can be attributed to the starting of the plastic flow and the shear mechanisms of the material under study and further mechanical and micro-structural investigations must be carried out in order to highlight the alteration of the microstructure into this zone of transition.

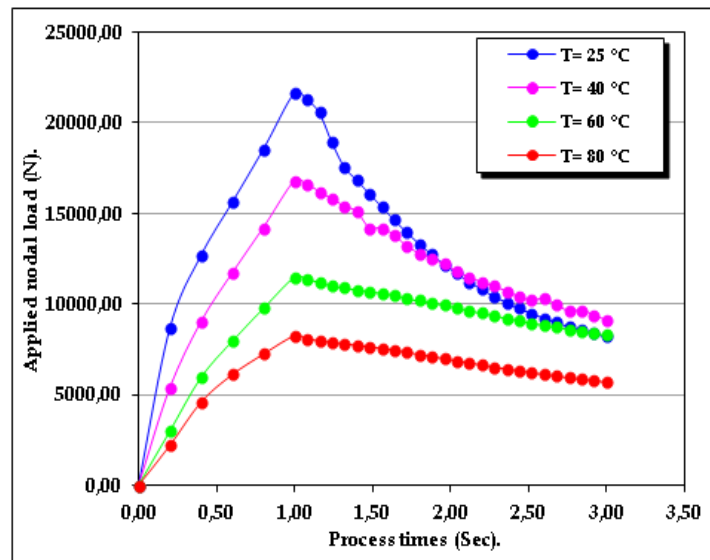


Figure 11. Evolution of the applied load during HPT process for different temperatures

Evolution of the Torsion Moment

Figure 12 shows the evolution of the torsion moment (torque) as a function of the time during HPT process for the various temperatures (25, 40, 60 and 80°C).

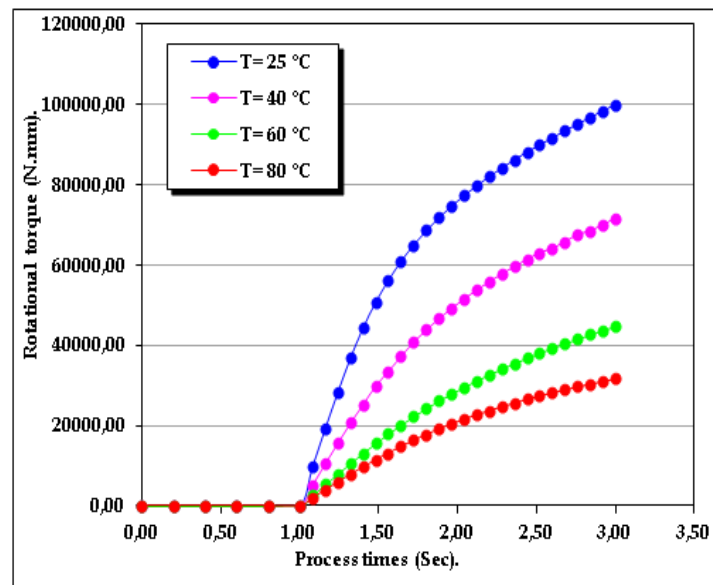


Figure 12. Evolution of the rotational torque during HPT process for different temperatures

It can be seen that the torque begins to increase at the triggering of the torsion phase and is inversely proportional to the temperature increase (the higher is the temperature, the lower is the torque). Consequently, if there will be a limitation of the machine, one can increase the material temperature in order to reduce the magnitude of the pressing force and the torsion moment. Indeed, for the temperatures of (25, 40, 60 and 80°C), the maximum torques are respectively (100, 71.6, 44.7, and 31.6 kN.mm). Indeed, it can be observed that the torque at $T = 25^{\circ}\text{C}$ is about three times of that at $T = 80^{\circ}\text{C}$.

Conclusion

In this study the results of the elastic-viscoplastic finite element analysis of HDPE during HPT process under different temperatures were investigated. The effect of the sample thickness on the equivalent plastic strain distribution has been also analyzed. The following concluding remarks can be drawn:

- The equivalent plastic strain decreases with the increase of the sample thickness and the non-uniform plastic strain is more pronounced in the radial direction compared to that of the axial direction. So, in order to obtain a good homogeneity with high level of plastic strain, it is advised to conduct HPT process on samples with low thicknesses.
- The temperature of the process has a significant influence on the magnitude of the plastic strain and the required loadings (pressing force and torsion moment). A temperature increase leads to lower plastic strain in the sample and a significant reduction of the required pressing force and torsion moment.

Finally, in order to highlight the evolution of the mechanical properties and the microstructure alteration, experimental analyzes of HPT process must be carried out and work on these aspects are under investigation.

Acknowledgments

Support for this work has been provided by the Mechanical Laboratory of Lille, (France). The authors especially thank Profs. Moussa Nait-Abdelaziz, Jean-Michel Gloaguen and Pr. Fahmi Zaïri from Polytech'Lille, for their assistance in the compressive tests and parameters identification.

References

- B. Aour, F. Zaïri, J.M. Gloaguen, M. Naït-Abdelaziz, & J.M. Lefebvre, (2008). "A computational study of die geometry and processing conditions effects on equal channel angular extrusion of a polymer", *Int. J. Mech. Sci.*, vol. 50, pp. 589-602.
- B. Aour, F. Zaïri, J.M. Gloaguen, M. Naït-Abdelaziz, & J.M. Lefebvre, (2009). "Finite element analysis of plastic strain distribution in multi-pass ECAE process of high density polyethylene", *J. Manuf. Sci. Eng. ASME.*, vol. 131, no. 3, pp. 031016-11.

- B. Aour, F. Zaïri, J.M. Gloaguen, M. Naït-Abdelaziz, & J.M. Lefebvre, (2010). "Analysis of polypropylene deformation in a 135° ECAE die: experiments and three-dimensional finite element simulations", *Key. Eng. Mater.*, vol. 423, pp. 71-78.
- M.C. Boyce, S. Socrate, & P.G. Llana, (2000). "Constitutive model for the finite deformation stress-strain behavior of poly(ethylene terephthalate) above the glass transition", *Polym.*, vol. 41, pp. 2183-2201.
- A. Draï, & B. Aour, (2013). "Analysis of plastic deformation behavior of HDPE during high pressure torsion process", *Engineering Structures*, vol. 46, pp. 87-93.
- J.Y. Huang, Y.T. Zhu, H. Jiang, & T.C. Love, (2001). "Microstructure and dislocation configuration in nanostructured Cu processed by repetitive corrugation and straightening", *Acta Materialia*, vol. 49, pp. 1497-1505.
- S. Kobayashi, S.I. Oh & T. Altan, (1988). "Metal Forming and the Finite-Element Method", 1st ed., Oxford University Press, New York, USA.
- D. Mousumi, D. Goutam, G. Mainak, W. Matthias, V. Rajnikant & C.S. Ghosh, (2012). "Microstructures and mechanical properties of HPT processed 6063 Al alloy", *Materials Science & Engineering*, vol. A558, pp. 525-532.
- J. Richert, & M. Richert, (1986). "A new method for unlimited deformation of metals and alloys", *Aluminium*, vol. 62, no.8, pp. 604-607.
- Y. Saito, H. Utsunomiya, N. Tsuji, & T. Sakai, (1999). "Novel ultra-high straining process for bulk materials development of accumulative roll-bonding (ARB) process", *Acta Mater.*, vol. 47, pp. 579-583.
- V.M. Segal, (1995). "Materials Processing by simple shear", *Mater. Sci. Eng.*, vol. A 197, pp. 157-164.
- B. Srinivas, C. Srinivasu, B. Mahesh & M.A. Aqheel, (2013). "Review on Severe Plastic Deformation", *Adv. Mater. Manufacturing & Characterization*, vol. 3, no. 1, pp. 291-296.
- T.A. Tervoort, R.J.M. Smit, W.A.M. Brekelmans, & L. Govaert, (1998). "A constitutive equation for the elasto-viscoplastic deformation of glassy polymers", *Mech. Time-Depend. Mater.*, vol. 1, pp. 269-291.
- R.Z. Valiev, R.K. Islamgaliev, & I. V. Alexandrov, (2000). "Bulk Nanostructured Materials from Severe Plastic Deformation", *Prog. Mater. Sci.*, vol. 45, 103-189.